Delft University of Technology

Design, Control, and Evaluation of a Photovoltaic Snow Removal Strategy Based on a Bidirectional DC-DC Converter for Photovoltaic–Electric Vehicle Application

Hesham Ashraf Saeed Mohamed Saad Sharaf, Hesham; Bastawrous, H.; Makeen, Peter

DOI
10.3390/en17246468

Publication date
2024

Document Version
Final published version

Published in
Energies

Citation (APA)
Hesham Ashraf Saeed Mohamed Saad Sharaf, H., Bastawrous, H., & Makeen, P. (2024). Design, Control, and Evaluation of a Photovoltaic Snow Removal Strategy Based on a Bidirectional DC-DC Converter for Photovoltaic–Electric Vehicle Application. *Energies*, *17*(24), Article 6468. https://doi.org/10.3390/en17246468

Important note
To cite this publication, please use the final published version (if applicable).
Please check the document version above.

Copyright
Other than for strictly personal use, it is not permitted to download, forward or distribute the text or part of it, without the consent of the author(s) and/or copyright holder(s), unless the work is under an open content license such as Creative Commons.

Takedown policy
Please contact us and provide details if you believe this document breaches copyrights.
We will remove access to the work immediately and investigate your claim.

This work is downloaded from Delft University of Technology.
For technical reasons the number of authors shown on this cover page is limited to a maximum of 10.

energies

MDPI

Article

Design, Control, and Evaluation of a Photovoltaic Snow Removal Strategy Based on a Bidirectional DC-DC Converter for Photovoltaic–Electric Vehicle Application

Salma Elakkad [1], Mohamed Hesham [1], Hany Ayad Bastawrous [2,*] and Peter Makeen [1]

[1] Electrical Engineering Department, Faculty of Engineering, The British University in Egypt (BUE), Cairo 11837, Egypt; salma.elakkad@bue.edu.eg (S.E.); mohamed195789@bue.edu.eg (M.H.); peter.makeen@bue.edu.eg (P.M.)

[2] Department of Microelectronics, Faculty of Electrical Engineering, Mathematics and Computer Science, Delft University of Technology (TU Delft), 2628CD Delft, The Netherlands

* Correspondence: h.bastawrous@tudelft.nl

Abstract: A novel self-heating technique is proposed to clear snow from photovoltaic panels as a solution to the issue of winter snow accumulation in photovoltaic (PV) power plants. This approach aims to address the shortcomings of existing methods. It reduces PV cell wear, resource loss, and safety risks, without the need for additional devices. A self-heating current is applied to the solar panel to melt the snow covering its surface, which is then allowed to slide off the panel due to gravity. The proposed system consists of a bidirectional DC-DC converter, which removes the snow cover by heating the solar PV modules using electricity from the grid or electric vehicle (EV) batteries. It also charges the EV battery pack and/or supplies the DC bus when no EV is plugged into the charging station. For each mode of operation, a current-controlled system was implemented using a PI controller and a model predictive controller (MPC). The MPC approach achieved a faster rise time, shorter settling time, very low current ripples, and high stability for the proposed system. Specifically, the settling time decreased from 9 ms and 155 ms when using the PI controller at 20 μs and 35 μs with the MPC controller for both the buck and boost modes, respectively.

Keywords: bidirectional converter; buck converter; boost converter; PV cells; electric vehicles

Academic Editor: Anastassios M. Stamatelos

Received: 2 December 2024
Revised: 18 December 2024
Accepted: 20 December 2024
Published: 22 December 2024

Citation: Elakkad, S.; Hesham, M.; Bastawrous, H.A.; Makeen, P. Design, Control, and Evaluation of a Photovoltaic Snow Removal Strategy Based on a Bidirectional DC-DC Converter for Photovoltaic–Electric Vehicle Application. *Energies* **2024**, *17*, 6468. https://doi.org/10.3390/en17246468

Copyright: © 2024 by the authors. Licensee MDPI, Basel, Switzerland. This article is an open access article distributed under the terms and conditions of the Creative Commons Attribution (CC BY) license (https://creativecommons.org/licenses/by/4.0/).

1. Introduction

In recent years, the rapid expansion of renewable energy sources, such as photovoltaics (PVs), has posed challenges to the efficient operation of power grids. The fluctuations in renewable energy source (RES) output can be mitigated by integrating energy storage devices. However, the widespread adoption of energy storage has been hindered by high costs and safety concerns. With advancements in coordinated electric vehicle (EV) charging and discharging technologies, EV charging stations are beginning to exhibit functionalities similar to energy storage systems. Furthermore, as the number of EVs continues to grow, the scale of EV charging infrastructure is expected to increase substantially as well [1–3]. Studies have demonstrated the potential of various RESs for global energy consumption, with solar energy being the most promising [4]. However, the impact of solar energy on power generation remains limited due to several constraints, including high costs, energy storage issues, and efficiency challenges [5].

In high-latitude regions during the winter, ice and snow accumulation on solar panels can severely reduce energy efficiency if not promptly removed or melted. Thick layers of snow can freeze on the surface of PV panels, preventing direct exposure to sunlight. This can lead to no energy production for long periods until the temperature rises enough to naturally melt the snow, reducing electrical generation by 90% to 100% during the winter season.

To address this issue, many researchers have proposed both passive and active solutions over the decades [5–7]. Soltek Solar Energy Ltd. [8] constructed a passive solution using flush-mounted panels that help reduce the accumulation of ice on solar modules. However, this solution was unable to eliminate the problem entirely. In 1995, another passive heating system was proposed by Ross and Usher [9], which used a black foil to absorb radiation reflected from the snow-covered ground. This heat was transferred to the back surface of the PV module, but the results were not promising. Several studies have also proposed active solutions. Research from 2003 to 2014 showed that the pn junction characteristics of the diode in the PV cell could be used to function both as a power source and a load [10–12]. This was implemented by Jianan et al. in their study, which modeled the PV solar cell as a resistive load when covered by snow, due to the lack of irradiance and sun exposure [13]. A system using the internal pn junction characteristics of PV cells to melt snow was investigated in [14]. The results showed a temperature rise of 16.5 Kelvin, producing a current of 2.2 A in an air environment without snow. A thin metal foil heater was added to address the issue of the solar panel aluminum frame preventing the snow from sliding off the panels. This led to a heating time of approximately 15 min, at which point the snow began to slide off the PV modules. However, these experiments were conducted with manually placed snow and did not test real-world snow conditions. In 2020, Chenyue Yan et al. explained how a current with exponential dependence could be established within the device upon the application of a specific positive potential difference to the PV cell [15]. During this process, the PV cell behaves as a load in the circuit. Heat is produced within the semiconductor region of the PV module, which can be used to melt the snow and cause it to slide down the panel naturally by gravity. The results showed that it took 91.1 min (of which 20.1 min were mainly for heating) to melt a 4 cm thick snow layer. Interestingly, this time decreased for thicker layers of snow, such that it took 65.2 min (of which 11.9 min were for heating) to remove an 8 cm thick snow layer. These experiments demonstrate the feasibility of this method at middle to high latitudes. In [16], the authors explored snow removal by generating reverse currents through PV cells. The study focused on the influence of various parameters, such as tilt angle, solar irradiance, ambient temperature, and wind speed. The findings also verified that using reverse current through PV cells is more energy-efficient than conventional heaters.

Bidirectional DC-DC converters are employed in RESs, smart grids, and EV charging stations. In the vehicle-to-grid (V2G) architecture, these converters charge EVs from the power grid and feed the energy stored in EV batteries back to the grid when necessary. Therefore, bidirectional DC-DC converters with low cost, high efficiency, and high reliability are crucial components for EV charging stations. The applications and controllers of bidirectional power converters extend beyond just EVs, as mentioned in [17–21]. Since the DC-DC converter is an integral part of the PV system, improving its performance is of high importance. Multiple controllers have been studied to optimize DC-DC converter performance for various applications. In [22], the authors focused on the proportional–integral (PI) controller for DC-DC converters. In [23], a comparison of PID controller tuning methods for DC-DC converters was investigated. An interesting study proposed in [24] used model predictive control (MPC) for maximum power point tracking (MPPT) and voltage regulation of DC-DC converters in solar PV systems, concluding that this approach offers fast response and low output ripples.

While the aforementioned studies highlight the potential of reverse current-based snow removal and the investigation of controllers for DC-DC converters, a critical research gap remains in comprehensively investigating the influence of these controllers and their parameters on the process of mode control for melting accumulated snow on PV panels.

In this work, a controlled bidirectional DC-DC buck–boost converter is used to facilitate direct current flow to a battery pack for charging an EV, while also enabling reverse current flow to heat the PV cells and melt snow accumulated on the panels during the cold winter season. The system utilizes power from the EV battery pack for this process. Additionally, various case studies are proposed and investigated while implementing different controllers. The system's behavior in both buck and boost modes is analyzed using a PI controller implemented in MATLAB/Simulink R2022a to study transient effects. Furthermore, the discrete transfer function is controlled in both modes to obtain more effective results using both the MPC and PI controllers, as discussed in the following subsections. The proposed hierarchical controller based on MPC demonstrates robustness, reliability, and efficient dynamic response, as will be introduced in the following sections.

2. Proposed System

2.1. Overall System Construction

The proposed bidirectional DC-DC converter is illustrated in Figure 1a. It has two different modes: the buck mode and the boost mode. The buck mode is responsible for charging the EV from the PV system, while the boost mode generates a reverse current to heat the solar panels using energy from the EV battery pack. Both the buck and boost converters are designed to regulate the current and voltage to ensure the safety of both the PV system and the EV battery.

The boost mode is activated whenever there is snow or freezing rain, and the PV system requires a reverse current to heat the cells, either from the EV or the DC bus, as shown in the flowchart in Figure 1b. The buck mode is activated when power is generated by the PV system and is used to charge the EV or supply the DC bus, as indicated in the flowchart in Figure 1b.

Thus, if the EV is connected to the charging station and the PV system's power reaches 1 kW, the buck mode will successfully charge the EV battery. In contrast, if the following four conditions are met, (1) the PV output power falls below the predetermined threshold (1 kW); (2) it is snowing; (3) the EV battery's state of charge (SOC) is greater than 45%; and (4) the EV owner agrees to engage in the operation, the boost mode can be used to heat the PV solar panels.

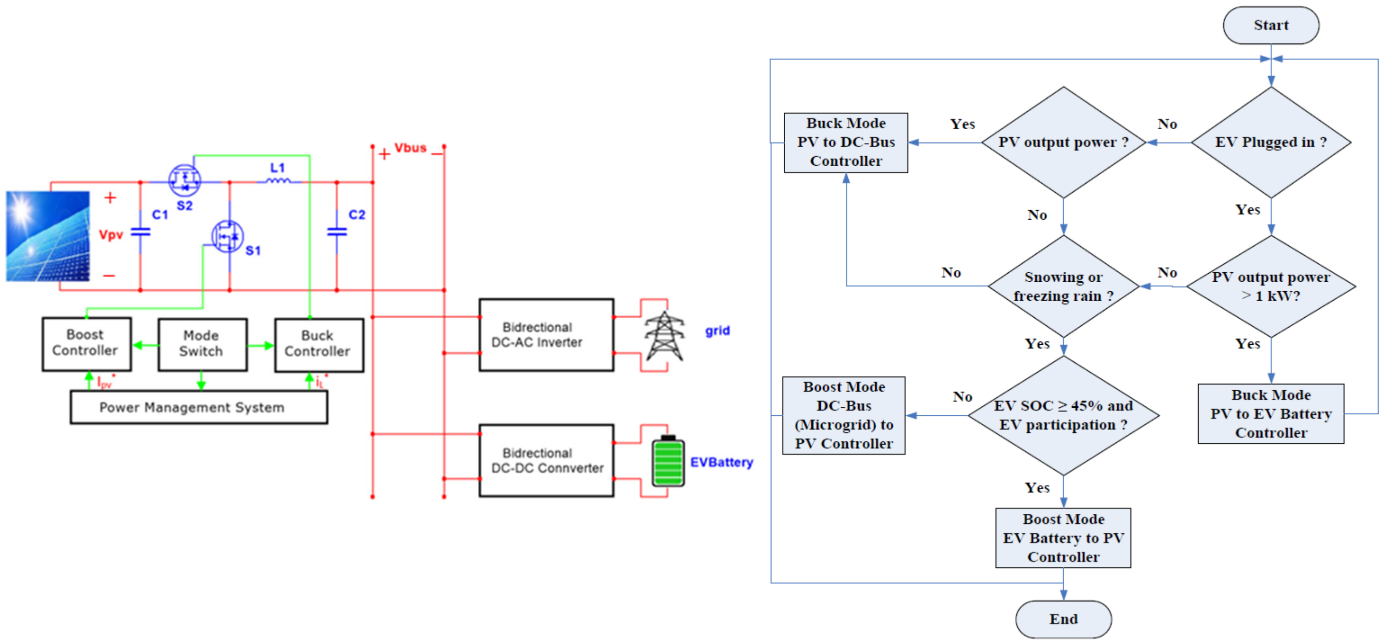

(**a**) (**b**)

Figure 1. (**a**) The proposed bidirectional converter. (**b**) Flowchart of the operational modes.

It is assumed that the power of the PV system is 26.113 kW, with a short-circuit current (SCC) of 35.82 A and an open-circuit voltage (OCV) of 729 V, where SunPower panels of the SPR-435NE-WHT-D model were used in the MATLAB/Simulink simulation. The array consists of 10 series modules and 6 parallel strings, and the I-V and P-V characteristics of the PV array are illustrated in Figure 2a.

The constant current constant voltage (CC-CV) charging protocol is the traditional method for EV battery charging. In comparison to the CC-CV approach, researchers are exploring methods to shorten charging times and reduce battery degradation. The battery is charged using a multi-stage application of various currents under the multi-stage charging protocol, extending its lifespan without causing deterioration. For multi-stage constant current charging of EV batteries, numerous algorithms and methods have been developed to shorten charging times, minimize energy loss, and improve charging efficiency, as shown in our previous work [25,26], and as depicted in Figure 2b. Hence, the main parameter to consider when charging the EV battery is the charging current, which is the backbone of our proposed controller. The parameters utilized in the proposed system are shown in Table 1.

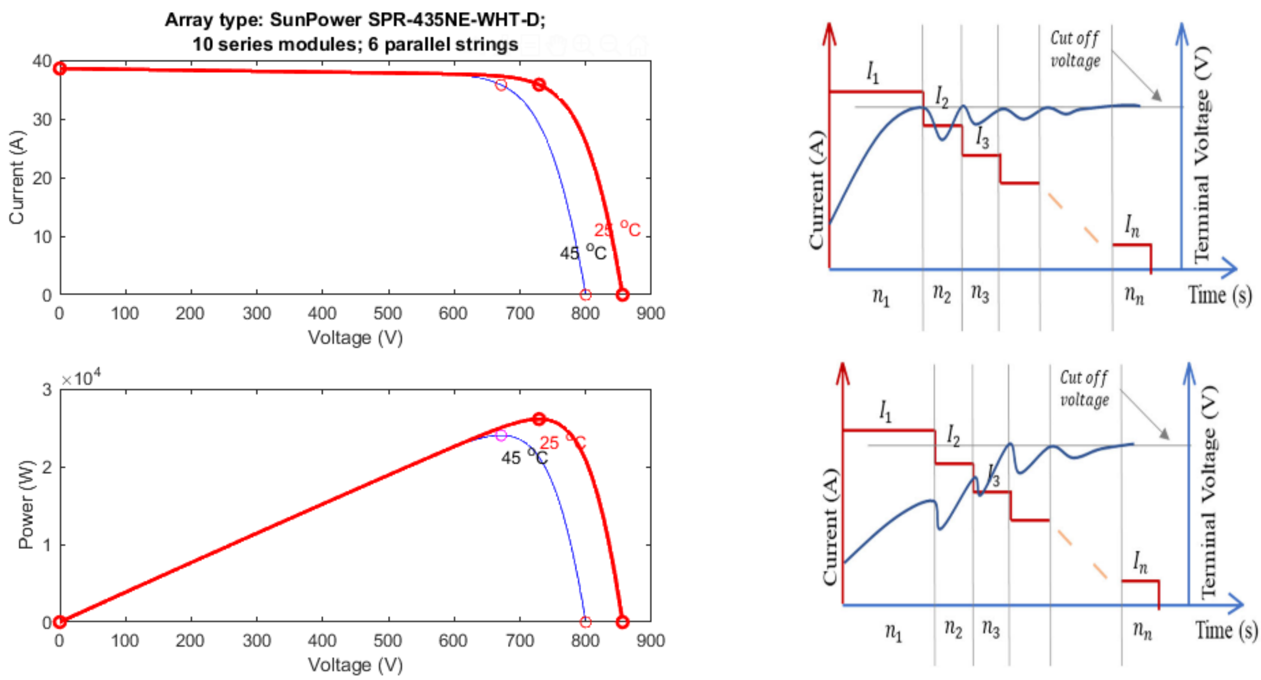

(**a**) (**b**)

Figure 2. (**a**) I-V and P-V characteristics of the PV array. (**b**) The charging current stage changes whenever the battery voltage reaches the cut-off value in different charging protocols.

Table 1. The parameters of the proposed system.

Parameter	Value
PV Nominal Voltage (V_1)	729 V
EV Nominal Voltage (V_2)	360 V
Maximum Input Current $\left(I_{1\,(Max)}\right)$	35.82 A
Nominal EV Discharging Current (A)	65.2174 A
EV Rated Capacity	150 Ah
EV SOC	45%
Power Rating	26.113 kW
Efficiency (η)	95%
Inductance (L)	13 mH
EV Capacitance (C_2)	20 µF
PV Capacitance (C_1)	1 mF
Switching Frequency (f_s)	30 kHz
Output and Input Voltage Variations	1%

2.2. Design of the Proposed Bidirectional DC-DC Converter

2.2.1. Mode 1: Boost Mode Mathematical Model

The boost operational mode circuit is presented in Figure 3. The solar PV panel is represented by a load denoted as (R_{pv}) where its calculation process is explained in detail in this section. The EV battery pack is represented by a voltage source denoted as (V_{bus}). The capacitance denoted as (C_2) can be neglected since it imposes no dynamic effect when there is a regulated voltage at the output port (V_{bus} is constant). The methodology used to obtain the mathematical modeling was adopted from [27].

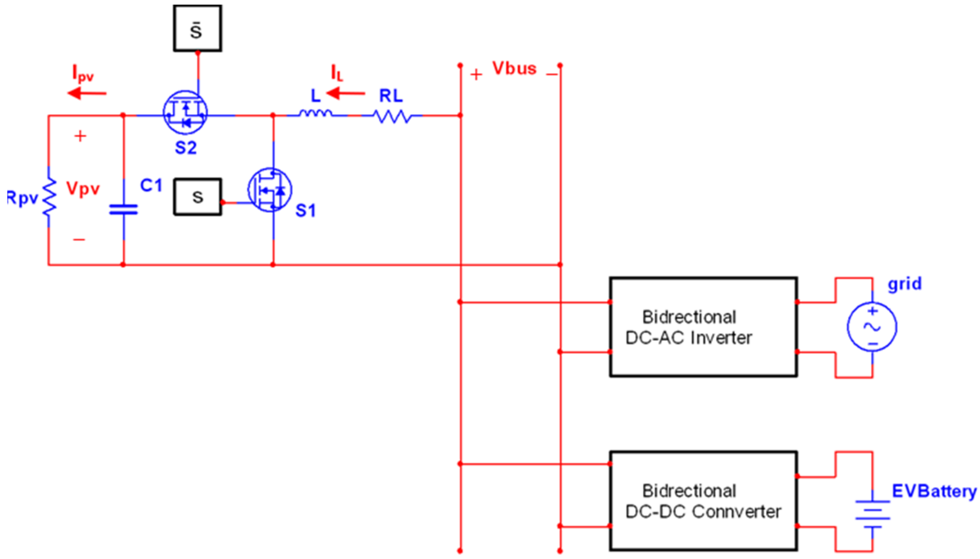

Figure 3. Boost mode operation circuit in the proposed bidirectional system.

Based on the boost converter representation shown in Figure 3, the EV battery current can be considered equivalent to the inductor current, as described in Equation (1). Additionally, the PV voltage and duty cycle of the proposed converter are represented by Equations (2) and (3), respectively. The mathematical model begins with the application of the state-space averaging method, from which three components of the model are derived, as shown in Equation (4). These components, discussed in detail in [27], are the equilibrium point, the linear dynamic component, and the nonlinear dynamic component. Therefore, the dynamic variables of the converter, in relation to the duty cycle, are obtained as shown in Equation (7).

$$I_L = I_{EV}, \tag{1}$$

$$V_{C1} = I_{EV} \cdot R_{EV}, \tag{2}$$

$$D = 1 - I_{EV}\left(\frac{R_{EV} + R_L}{V_{PV}}\right), \tag{3}$$

$$\begin{aligned} L\frac{di_L(t)}{dt} = {} & [V_{PV}(1-D)] - [I_L \cdot \alpha] - [V_{C1} \cdot \beta] + [V_{PV}(1-D)] - [i_L \cdot \alpha] \\ & - [V_{C1} \cdot \beta] - [dV_{PV}] - [V_{PV} d], \end{aligned} \tag{4}$$

$$C_1\frac{dV_{C1}(t)}{dt} = [I_L \cdot R_{EV} \cdot \gamma] - [V_{C1} \cdot \gamma] + [i_L \cdot R_{EV} \cdot \gamma] - [V_{C1} \cdot \gamma], \tag{5}$$

$$\begin{cases} \alpha = R_L + \dfrac{R_{EV} \cdot R_{C1}}{R_{EV} + R_{C1}} \\ \beta = 1 - \dfrac{R_{C1}}{R_{EV} + R_{C1}} \\ \gamma = \dfrac{1}{R_{EV} + R_{C1}} \end{cases}, \tag{6}$$

$$G_{id-Boost}(s) = \frac{I_L(s)}{D(s)} = \frac{\frac{-V_{PV} \cdot (C_1 \cdot s + \gamma)}{L \cdot C_1}}{s^2 + \frac{L \cdot \gamma + C_1 \cdot \alpha}{L \cdot C_1}s + \frac{R_{EV} \cdot \gamma \cdot \beta}{L \cdot C_1}}, \tag{7}$$

It is clear from the derived expressions in Equation (7) that the negative sign is due to the presence of a zero located on the right side of the plane. Finally, after deriving the final expression for the boost mode, a controller is used to regulate the inductor current. All the parameter values in Equation (7) are taken from Table 1.

2.2.2. Mode 2: Buck Mode Mathematical Model

The buck operational mode circuit is presented in Figure 4. The solar PV panel is represented by the Norton equivalent model, as mentioned in [27], where the equivalent PV resistance is assumed to be 395.64 Ω. The EV battery pack is represented by a voltage source denoted as (V_{bus}). Similarly, the capacitance (C_1) could be neglected as it imposes no dynamic effect when there is a regulated voltage at the output port.

The methodology used to obtain the mathematical modeling was adopted from [28], where the system was expressed as a third-order system with the following equation:

$$G_{id} = \frac{\hat{\imath}_L}{\widehat{D}} = \frac{(\alpha \cdot s + 1) \cdot [(\beta \cdot s + 1) \cdot V_{PV} - \gamma]}{(L \cdot s + R_L)(\alpha \cdot s + 1)(\beta \cdot s + 1) + D^2 R_{PV}(\alpha \cdot s + 1) + R_{EV}(\beta \cdot s + 1)}, \tag{8}$$

$$\begin{cases} \alpha = C_2 \cdot R_{EV} \\ \beta = C_{PV} \cdot R_{PV} \\ \gamma = D \cdot I_L \cdot R_{PV} \end{cases}, \tag{9}$$

The desired general formula for the buck mode controller, which also uses a controller to regulate the PV voltage, is now acquired. For a two-voltage-source system, the main transfer function can be represented in Equations (10) and (11), as investigated in [28].

$$I_L = \frac{D \cdot V_{PV} - V_{DC-Bus}}{R_L + R_{EV}}, \tag{10}$$

$$G_{id-Buck}(s) = \frac{\hat{\imath}_L}{\widehat{D}} = \frac{V_{PV}}{L \cdot s + R_L + R_{EV}}, \tag{11}$$

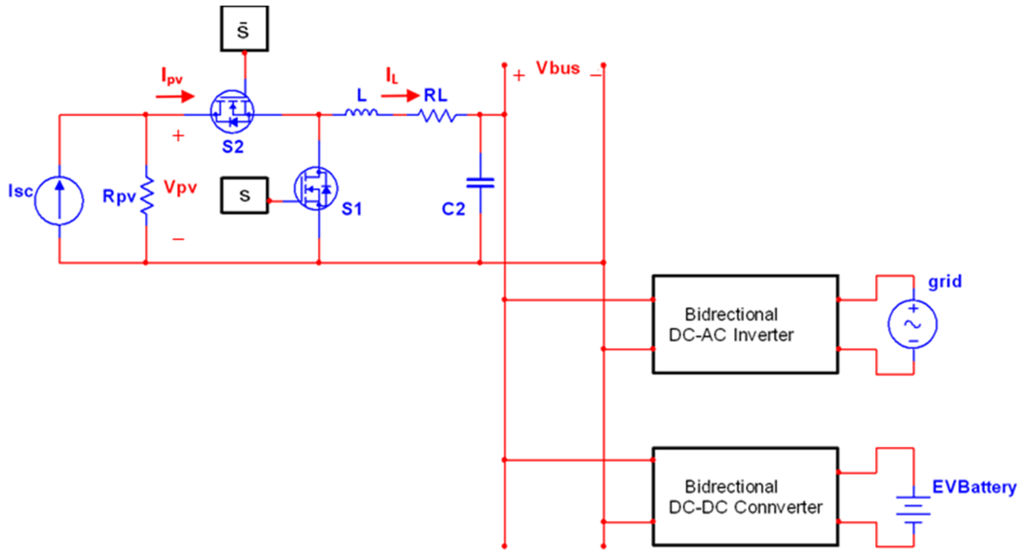

Figure 4. Buck mode operation circuit in the proposed bidirectional system.

2.2.3. Bidirectional DC-DC Converter Control System

After concluding the transfer function of the bidirectional DC-DC converter in both buck and boost modes, the equations were discretized using MATLAB. Then, different controllers were investigated to find the optimal dynamic behavior of the bidirectional converter.

The main proposed schematic diagram is presented in Figure 5. Figure 5a represents the boost mode, where the goal is to supply the PV with a specific reverse current to melt the snow on the panel. Figure 5b represents the buck mode, where the charging current for the EV is the main goal of the controller.

According to the literature, the PI controller is commonly used in bidirectional power converters. MATLAB/Simulink will automatically tune and generate the parameters that achieve the targeted behavior as per the controller's coefficients in Equation (12):

$$Controller_{PI}(z) = P + I \cdot T_s \frac{1}{z-1}, \quad (12)$$

where P and I are the proportional and integral coefficients, respectively, and T_s is the discrete sampling time, considered to be 5 μs.

One of the AI-based controllers used in other systems is the model predictive control (MPC), which can predict the future behavior of the system over a defined time range. Based on these predictions, the controller computes the best control parameters to meet the task objectives. It is worth noting that the MPC controller is used in various applications to sustain the stability and reliability of DC microgrids, as investigated in [29,30].

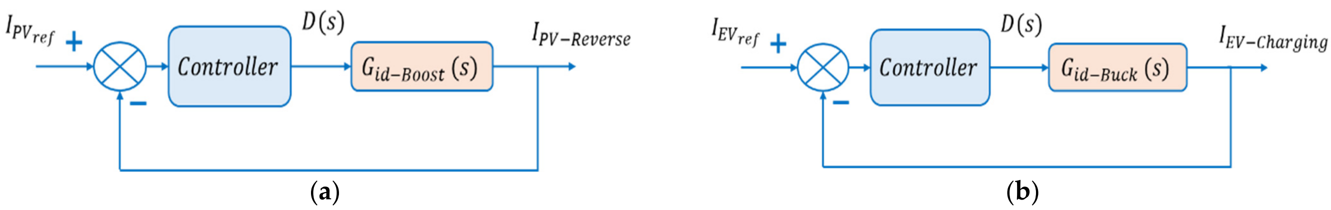

Figure 5. A schematic diagram of the proposed bidirectional system in both (**a**) boost and (**b**) buck modes.

3. Results and Discussion

3.1. Mode 1: Buck Mode Converter

The first mode is the buck mode converter, where the main goal is to charge the EV battery with a predetermined current, according to the EV battery specifications. The charging protocol depends entirely on the charging current, as shown in [25,26,31]. Controlling the charging current with minimal ripples and transient time is ensured, as shown in Figure 6a, where the settling time reached 4.17 ms and the peak-to-peak current ripple was 0.4621 A. The impact of the charging current on the EV battery is shown in Figure 6b. The input voltage and current of the PV panel are presented in Figure 7a. Additionally, different controllers, represented by the MPC and conventional PI, were implemented to achieve the optimal dynamic performance, as shown in Figure 7b. The parameters of the PI controller are 0.00987 and 0.01577, respectively, where the PI controller is optimized using MATLAB/Simulink auto-tuning based on the transfer function of the buck converter. The MPC controller implemented in this paper ensured a significant reduction in the transient response time of the system. This improvement is quantified by the observed settling time of 20.254 μs required to reach the desired steady-state value.

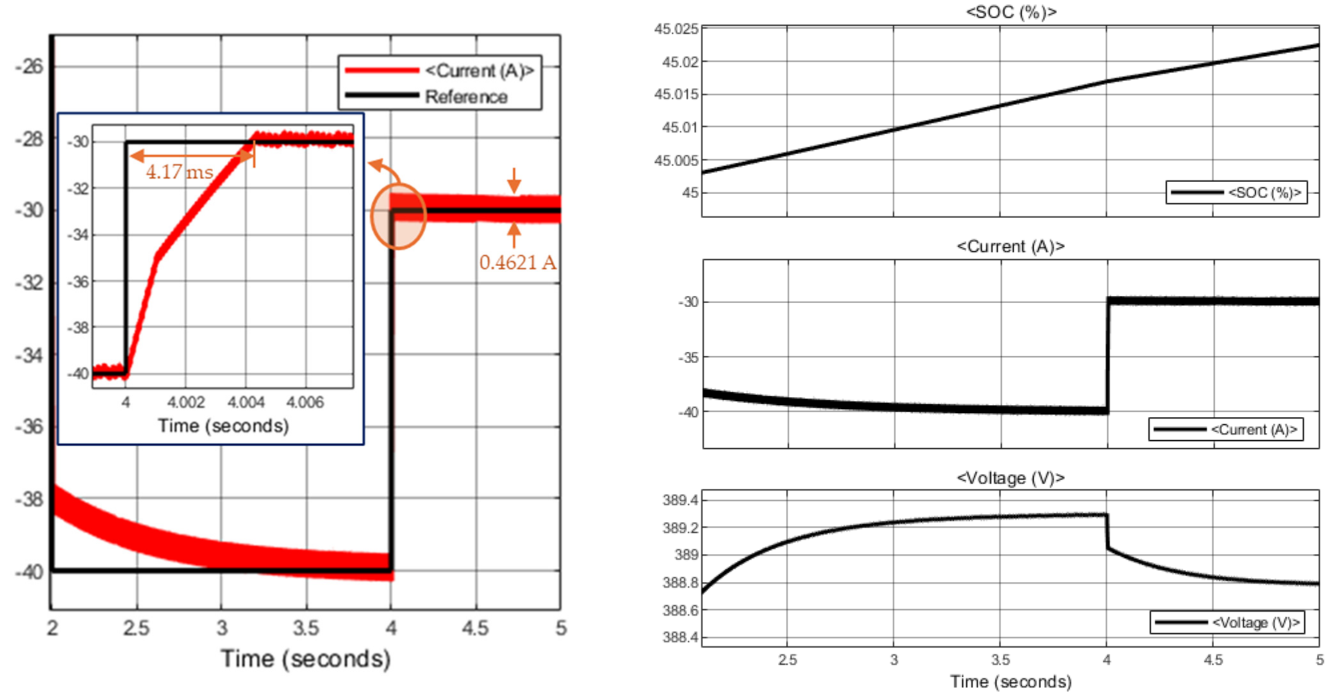

(**a**) (**b**)

Figure 6. Output results from the buck mode converter: (**a**) the charging current refers to the reference current and (**b**) EV battery SOC, current, and voltage while charging.

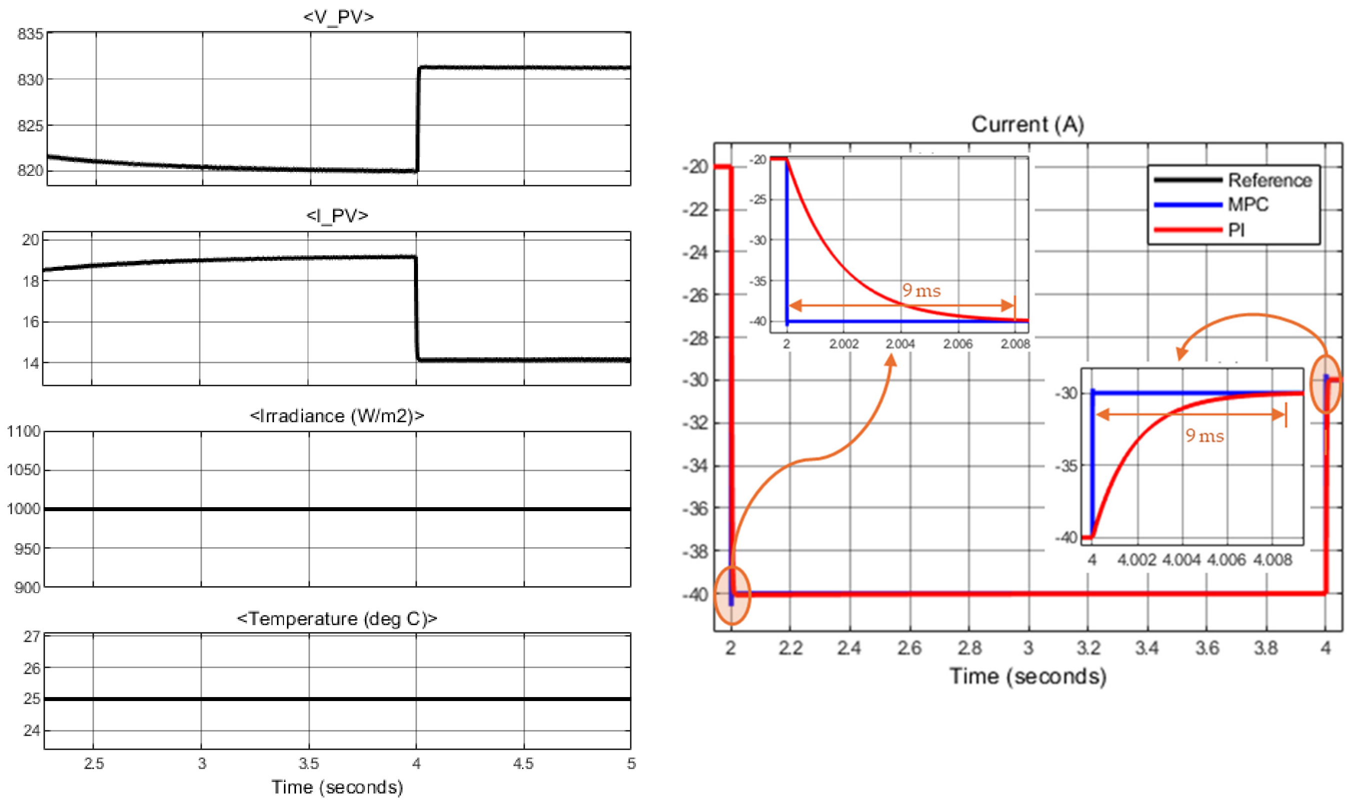

(**a**) (**b**)

Figure 7. Output results from the buck mode converter: (**a**) the PV current, voltage, irradiance, and temperature and (**b**) a comparison between the conventional PI controller and MPC controller.

3.2. Mode 2: Boost Mode Converter

The second mode is the boost mode converter, where the main goal is to heat the PV panel to remove the snow. Controlling the PV's reverse heating current with minimal ripples and transient time, while also controlling the EV discharging current according to the EV battery specifications, is ensured, as shown in Figure 8a. The settling time ranged from 800 ms to 125 ms while varying the reference current from 5 A to 7 A, with peak-to-peak current ripples of 0.021 A. The state of charge (SOC) of the EV battery during discharging is shown in Figure 8b. Different controllers, represented by the conventional PI controller and MPC controller, were implemented to achieve the optimal dynamic performance, as shown in Figure 9. The parameters of the PI controller are 0.002834 and 0.061532, respectively, where the PI controller is optimized using MATLAB/Simulink auto-tuning based on the transfer function of the boost converter. The MPC controller implemented in this paper ensured a significant reduction in the transient response time of the system. This improvement is quantified by the observed settling time of 35.421 μs required to reach the desired steady-state value.

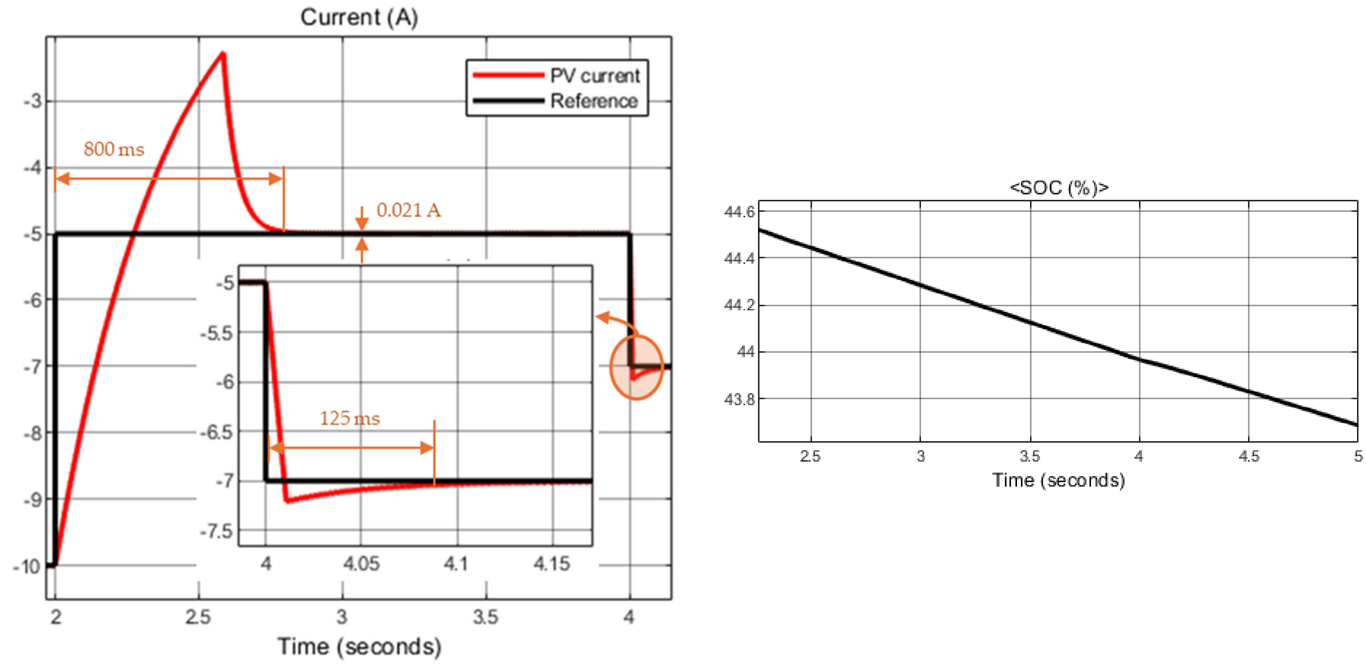

(**a**) (**b**)

Figure 8. Output results from the boost mode converter: (**a**) the reverse heating current refers to the discharging reference current and (**b**) EV battery SOC while discharging.

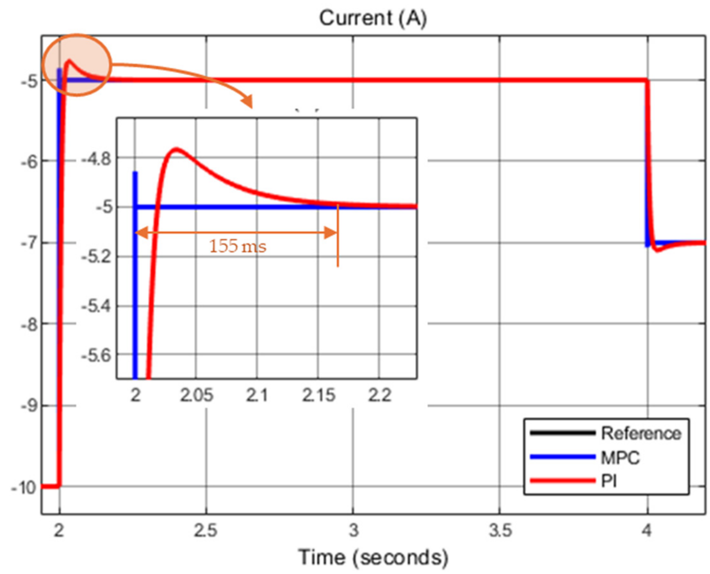

Figure 9. Comparison between the conventional PI controller and the AI-based MPC controller.

4. Conclusions

This paper introduces a novel snow removal approach to enhance the power generation efficiency of photovoltaic (PV) systems in snowy regions while charging EV batteries. This study systematically and comprehensively examines the feasibility, performance, and advantages of the proposed snow removal strategy. The goal is to explore the potential of snow removal strategies for large-scale practical applications, especially during EV battery charging. Various strategies are implemented in this paper under different scenarios to account for all possibilities. Additionally, different controllers are employed to achieve optimal transient behavior during both charging and discharging of the EV battery. Conventional PI and AI-based MPC controllers are implemented and compared. The MPC controller ensures shorter rise and settling times, lower current ripples, and greater robustness for the proposed system. It achieves a remarkable 99% reduction in settling time compared to the conventional PI controller, across both the buck and boost operating modes of the converter. The proposed hierarchical MPC-based controller demonstrates robustness, reliability, and efficient dynamic response, as will be discussed in the following sections. In future work, artificial intelligence-based controllers could be implemented in these subsystems and compared with the proposed controller under various environmental conditions, such as uneven snow distribution and varying tilt angles of the PV systems. Experimental studies could also assess the impact of charging and discharging protocols on EV battery lifespan. Additionally, future research could focus on system cost analysis, forecasting, and optimization.

Author Contributions: S.E. contributed to conceptualization, methodology, software, validation, writing—original draft preparation, writing—acquisition, writing—review and editing, and visualization; M.H. contributed to conceptualization, methodology, validation, writing—acquisition, and visualization; H.A.B. contributed to conceptualization, methodology, software, validation, writing—review and editing, visualization, supervision; and P.M. contributed to conceptualization, methodology, software, validation, writing—review and editing, visualization, supervision. All authors have read and agreed to the published version of the manuscript.

Funding: This research received no external funding.

Data Availability Statement: The original contributions presented in this study are included in the article. Further inquiries can be directed to the corresponding author.

Conflicts of Interest: The authors declare no conflicts of interest.

References

1. Sun, F.; Su, S.; Diao, R.; Cheng, H.; Meng, D.; Lu, S. Prediction-Based EV-PV Coordination Strategy for Charging Stations Using Reinforcement Learning. In Proceedings of the 2022 IEEE Transportation Electrification Conference and Expo, Asia-Pacific, ITEC Asia-Pacific 2022, Haining, China, 28–31 October 2022; Institute of Electrical and Electronics Engineers Inc.: Piscataway, NY, USA, 2022.
2. Li, L.-L.; Liu, Z.-F.; Tseng, M.-L.; Chiu, A.S. Enhancing the Lithium-Ion Battery Life Predictability Using a Hybrid Method. *Appl. Soft Comput. J.* **2019**, *74*, 110–121. https://doi.org/10.1016/j.asoc.2018.10.014.
3. Olabi, A.G.; Abdelghafar, A.A.; Maghrabie, H.M.; Sayed, E.T.; Rezk, H.; Radi, M.A.; Obaideen, K.; Abdelkareem, M.A. Application of Artificial Intelligence for Prediction, Optimization, and Control of Thermal Energy Storage Systems. *Therm. Sci. Eng. Prog.* **2023**, *39*, 101730.
4. Makeen, P.; Ghali, H.A.; Memon, S.; Duan, F. Smart Techno-Economic Operation of Electric Vehicle Charging Station in Egypt. *Energy* **2023**, *264*, 126151. https://doi.org/10.1016/j.energy.2022.126151.
5. Makeen, P.; Ghali, H.A.; Memon, S. Theoretical and Experimental Analysis of a New Intelligent Charging Controller for Off-Board Electric Vehicles Using PV Standalone System Represented by a Small-Scale Lithium-Ion Battery. *Sustainability* **2022**, *14*, 7396. https://doi.org/10.3390/su14127396.
6. Abou Yassine, A.H.; Khoshbakhtnejad, E.; Sojoudi, H. Economics of Snow Accumulation on Photovoltaic Modules. *Energies* **2024**, *17*, 2962. https://doi.org/10.3390/en17122962.
7. Abou Yassine, A.H.; Namdari, N.; Mohammadian, B.; Sojoudi, H. Understanding Mechanisms of Snow Removal from Photovoltaic Modules. *Sol. Energy* **2022**, *231*, 175–184. https://doi.org/10.1016/j.solener.2021.11.042.
8. Aragon Aviles, S.M. Design and Development of a Novel DC/DC Bidirectional Converter with Dual Solar/PV-Based Snow Removal and EV Charging Functionality. Master's Thesis, University of Ontario Institute of Technology, Oshawa, ON, Canada, 2022.
9. Ross, M.M.D.; Usher, E.P. Photovoltaic Array Icing and Snow Accumulation: A Study of a Passive Melting Technology. In Proceedings of the 21st Annual Conference of the Solar Energy Society of Canada, Toronto, ON, Canada, 31 October–2 November 1995; pp. 21–26.
10. Borrebæk, P.-O.A.; Jelle, B.P.; Zhang, Z. Avoiding Snow and Ice Accretion on Building Integrated Photovoltaics–Challenges, Strategies, and Opportunities. *Sol. Energy Mater. Sol. Cells* **2020**, *206*, 110306. https://doi.org/10.1016/j.solmat.2019.110306.
11. Rathore, N.; Panwar, N.L.; Yettou, F.; Gama, A. A Comprehensive Review of Different Types of Solar Photovoltaic Cells and Their Applications. *Int. J. Ambient Energy* **2021**, *42*, 1200–1217.
12. Al-Ezzi, A.S.; Ansari, M.N.M. Photovoltaic Solar Cells: A Review. *Appl. Syst. Innov.* **2022**, *5*, 67.
13. Zheng, J.; Liu, W.; Cui, T.; Wang, H.; Chen, F.; Gao, Y.; Fan, L.; Omer, A.A.A.; Ingenhoff, J.; Zhang, X.; et al. A Novel Domino-like Snow Removal System for Roof PV Arrays: Feasibility, Performance, and Economic Benefits. *Appl. Energy* **2023**, *333*, 120554. https://doi.org/10.1016/j.apenergy.2022.120554.
14. Weiss, A.; Weiss, H. Photovoltaic Cell Electrical Heating System for Removing Snow on Panel Including Verification. In Proceedings of the 2016 IEEE International Conference on Renewable Energy Research and Applications (ICRERA), Birmingham, UK, 20–23 November 2016; pp. 995–1000. https://doi.org/10.1109/ICRERA.2016.7884484.
15. Yan, C.; Qu, M.; Chen, Y.; Feng, M. Snow Removal Method for Self-Heating of Photovoltaic Panels and Its Feasibility Study. *Sol. Energy* **2020**, *206*, 374–380. https://doi.org/10.1016/j.solener.2020.04.064.
16. Rahmatmand, A.; Harrison, S.J.; Oosthuizen, P.H. An Experimental Investigation of Snow Removal from Photovoltaic Solar Panels by Electrical Heating. *Sol. Energy* **2018**, *171*, 811–826. https://doi.org/10.1016/j.solener.2018.07.015.
17. Trinh, H.-A.; Nguyen, D.G.; Phan, V.-D.; Duong, T.-Q.; Truong, H.-V.; Choi, S.-J.; Ahn, K.K. Robust Adaptive Control Strategy for a Bidirectional DC-DC Converter Based on Extremum Seeking and Sliding Mode Control. *Sensors* **2023**, *23*, 457. https://doi.org/10.3390/s23010457.
18. Danyali, S.; Shirkhani, M.; Tavoosi, J.; Razi, A.G.; Salah, M.M.; Shaker, A. Developing an Integrated Soft-Switching Bidirectional DC/DC Converter for Solar-Powered LED Street Lighting. *Sustainability* **2023**, *15*, 15022. https://doi.org/10.3390/su152015022.
19. Gorji, S.A.; Sahebi, H.G.; Ektesabi, M.; Rad, A.B. Topologies and Control Schemes of Bidirectional DC–DC Power Converters: An Overview. *IEEE Access* **2019**, *7*, 117997–118019. https://doi.org/10.1109/ACCESS.2019.2937239.
20. Latin, I.; Transactions, A. Review of Bidirectional DC-DC Converters and Trends in Control Techniques for Applications in Electric Vehicles. *IEEE Lat. Am. Trans.* **2024**, *22*, 177–155.

21. Wang, Y.; Li, Y.; Guan, Y.; Xu, D. Topology and Control Optimization of Bidirectional DC/DC Converter for Electric Vehicles. *IEEE J. Emerg. Sel. Top. Power. Electron.* **2024**, *12*, 257–268. https://doi.org/10.1109/JESTPE.2023.3278718.
22. Prajapati, S.; Garg, M.M.; Prithvi, B. Design of Fractional-Order PI Controller for DC-DC Power Converters. In Proceedings of the 2018 8th IEEE India International Conference on Power Electronics (IICPE), Jaipur, India, 13–15 December 2018; pp. 1–6. https://doi.org/10.1109/IICPE.2018.8709430.
23. Ibrahim, O.; Yahaya, N.Z.; Saad, N. Comparative Studies of PID Controller Tuning Methods on a DC-DC Boost Converter. In Proceedings of the 2016 6th International Conference on Intelligent and Advanced Systems (ICIAS), Kuala Lumpur, Malaysia, 15–17 August 2016; pp. 1–5. https://doi.org/10.1109/ICIAS.2016.7824044.
24. Ma, M.; Liu, X.; Lee, K.Y. Maximum Power Point Tracking and Voltage Regulation of Two-Stage Grid-Tied PV System Based on Model Predictive Control. *Energies* **2020**, *13*, 1304. https://doi.org/10.3390/en13061304.
25. Makeen, P.; Ghali, H.A.; Memon, S. Experimental and Theoretical Analysis of the Fast Charging Polymer Lithium-Ion Battery Based on Cuckoo Optimization Algorithm (COA). *IEEE Access* **2020**, *8*, 140486–140496. https://doi.org/10.1109/ACCESS.2020.3012913.
26. Makeen, P.; Ghali, H.A.; Memon, S. A Review of Various Fast Charging Power and Thermal Protocols for Electric Vehicles Represented by Lithium-Ion Battery Systems. *Future Transp.* **2022**, *2*, 281–299.
27. Aragon-Aviles, S.; Kadam, A.H.; Sidhu, T.; Williamson, S.S. Modeling, Analysis, Design, and Simulation of a Bidirectional DC-DC Converter with Integrated Snow Removal Functionality for Solar PV Electric Vehicle Charger Applications. *Energies* **2022**, *15*, 2961. https://doi.org/10.3390/en15082961.
28. Zhang, J.; Lai, J.-S.; Yu, W. Bidirectional DC-DC Converter Modeling and Unified Controller with Digital Implementation. In Proceedings of the 2008 Twenty-Third Annual IEEE Applied Power Electronics Conference and Exposition, Austin, TX, USA, 24–28 February 2008; pp. 1747–1753. https://doi.org/10.1109/APEC.2008.4522963.
29. Shan, Y.; Hu, J.; Chan, K.W.; Fu, Q.; Guerrero, J.M. Model Predictive Control of Bidirectional DC-DC Converters and AC/DC Interlinking Converters—A New Control Method for PV-Wind-Battery Microgrids. *IEEE Trans. Sustain. Energy* **2019**, *10*, 1823–1833. https://doi.org/10.1109/TSTE.2018.2873390.
30. Xu, Q.; Vafamand, N.; Chen, L.; Dragicevic, T.; Xie, L.; Blaabjerg, F. Review on Advanced Control Technologies for Bidirectional DC/DC Converters in DC Microgrids. *IEEE J. Emerg. Sel. Top. Power Electron.* **2021**, *9*, 1205–1221. https://doi.org/10.1109/JESTPE.2020.2978064.
31. Makeen, P.; Ghali, H.A.; Memon, S.; Duan, F. Impacts of Electric Vehicle Fast Charging under Dynamic Temperature and Humidity: Experimental and Theoretically Validated Model Analyses. *Energy* **2022**, *261*, 125335. https://doi.org/10.1016/j.energy.2022.125335.

Disclaimer/Publisher's Note: The statements, opinions and data contained in all publications are solely those of the individual author(s) and contributor(s) and not of MDPI and/or the editor(s). MDPI and/or the editor(s) disclaim responsibility for any injury to people or property resulting from any ideas, methods, instructions or products referred to in the content.